Identifying Error-Box Parameters from the Twelve-Term Vector Network Analyzer Error Model

S. Vandenberghe, D. Schreurs, G. Carchon*,
B. Nauwelaers, W. De Raedt*

K.U.Leuven ESAT TELEMIC, Kasteelpark Arenberg 10, B–3001 Leuven, Belgium.
*IMEC, Kapeldreef 75, B–3001 Leuven, Belgium

The following preprint differs from the final publication:

S. Vandenberghe, D. Schreurs, G. Carchon, B. Nauwelaers, W. De Raedt, "Identifying Error-Box Parameters from the Twelve-Term Vector Network Analyzer Error Model," *Automatic RF Techniques Group Conference (ARFTG),* Washington D.C., USA, December 2002, pp. 157–165.

Identifying Error-Box Parameters from the Twelve-Term Vector Network Analyzer Error Model

S. Vandenberghe, D. Schreurs, G. Carchon*,
B. Nauwelaers, W. De Raedt*

K.U.Leuven ESAT TELEMIC, Kasteelpark Arenberg 10, B–3001 Leuven, Belgium.
*IMEC, Kapeldreef 75, B–3001 Leuven, Belgium

Abstract— Two models describing the systematic measurement error in a two port vector network analyzer are in use. Conditions relating the twelve E-term error model and physically based eight S-term error box model are derived. Three practical E- to S-term conversion algorithms are presented. An example VNA test set is analyzed as to allow for measurement interpretation. Reported results show the limitations of each algorithm.

1 Introduction

Calibration of two port vector network analyzers (VNA) is a well known problem. All techniques determine the systematic measurement error of the equipment. Two types of mathematical error models are in use. The common twelve E-term description is employed for three sampler designs. Such VNAs only allow for the measurement of three waves at a time and require a separate forward and reverse stimulation error model.

The eight S-term error box model closely mimics the underlying equipment. It relates the four measured raw waves to true waves at the device under test (DUT) and is thus only applicable to four sampler VNA designs. It can be used for three sampler setups if the unmeasured wave is calculable somehow. An approach[1] is to model the internal termination of the unstimulated port. Three detector four sampler hybrid designs are capable of measuring these load reflections.

Clearly, the E-term model and S-term error box model, combined with the two load reflections, comprise the same information. This paper offers a detailed description of both models and its use. It further presents three methods of conversion, including an E-term based SOLT to SOLR conversion. Also, a VNA test set is described as to allow for interpretation of the measurement results.

The presented algorithms may be useful in general. Conversion from an E- to S-term model allows for a straightforward interpretation and verification, especially if the error boxes correspond to physical two-port devices. On the other hand, S- to E-term conversion is required if the model is to be used in most network analyzers.

2 The physical VNA error model

A VNA determines the scattering parameters of a two port device under test. This is done by applying the radio frequency (RF) power sequentially at port 1 and 2 with the unstimulated port terminated by a load[1], see fig. 1. Each excitation results in a set of two incident and two reflected waves at the test ports, and each set of waves relates the four raw S-parameters via two linear homogeneous equations. The two experiments, a forward (F) and reverse (R) stimulation, allow for the calculation of the raw DUT's response.

These waves can be measured using two couplers at each port, as is done in e.g. the Agilent 85110 110 GHz test set. Crosstalk in the measured transmitted waves b^F_{r2} and b^R_{r1} is assumed subtracted via the isolation terms and is not present in the physical model. The raw S-parameter response then follows from

$$\begin{bmatrix} b^F_{r1} & b^R_{r1} \\ b^F_{r2} & b^R_{r2} \end{bmatrix} = S_r \begin{bmatrix} a^F_{r1} & a^R_{r1} \\ a^F_{r2} & a^R_{r2} \end{bmatrix} \quad (1)$$

$$\Leftrightarrow S_r = B_r A_r^{-1} \quad (2)$$

where the reference impedances Z_{r1} and Z_{r2} are clearly set by the directional couplers.

The two error boxes S_a and S_b relate the raw to true waves, and consist of coupler imperfections, cables and connectors, and a reference impedance change, see fig. 1. The source and load reflection are outside of the error boxes and do not change this relation. These reflections will influence the actual value of the incident waves a_r during the forward and reverse measurement, and the final measurement accuracy since the two sets' linear independence determines the numerical stability when solving (1) for S_r. They also partially determine the impedances experienced by the DUT.

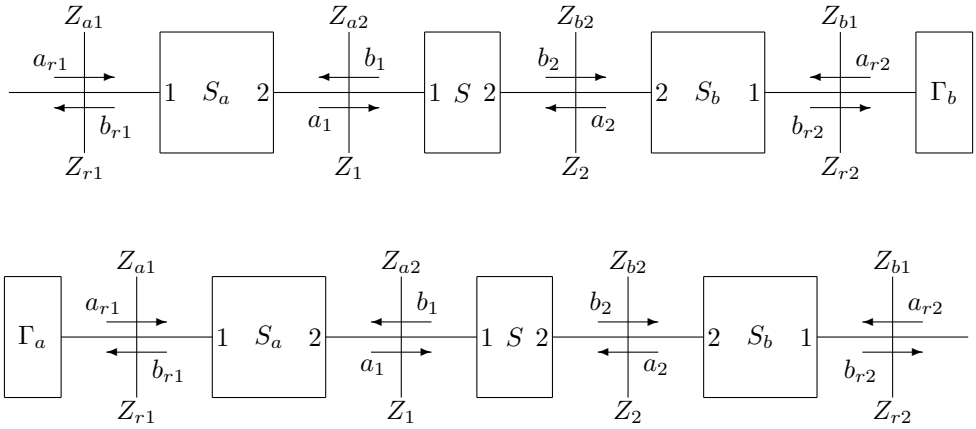

Figure 1: The physical forward and reverse model of a VNA. The raw applied and backscattered waves a_r and b_r are assumed corrected for crosstalk. Thus, the error box S_x unambiguously relates the port i raw and true waves. The measurement of two disjunct sets of four waves allows for the calculation of the raw S-parameters.

The true DUT S-parameter ratios are recovered via the deembedding of the error boxes S_a and S_b. An alternative is to calculate the DUT waves for the F/R measurement and to solve (1). The physical model is characterized by eight S-terms, but only seven parameters are needed for unambiguous S-parameter deembedding. Expressing S_r as the cascade of $S_a \| S \| \overline{S}_b$ shows that the result is unique if the four reflections S_{xii} and three out of the five quantities

$$k_1 = S_{a12}S_{a21} \qquad k_2 = S_{b12}S_{b21} \tag{3}$$
$$k_3 = S_{a21}S_{b12} \qquad k_4 = S_{a12}S_{b21} \tag{4}$$
$$r_{ab} = S_{a21}/S_{b21} = k_1/k_4 = k_3/k_2 \tag{5}$$

are known.

Converse, relative raw S-parameter based calibration techniques, like Thru-Line-Reflect, Line-Reflect-Match and Short-Open-Load-Reciprocal, only recover seven parameters. The error box completion algorithm for TLR[2][3][4], TMR/LRM[5], and SOLR[6], uses k_1, k_2, k_3, and the redundant k_4. The free unknown S_{a21} may be set to unity, or chosen for optimal reciprocity[1][7].

3 Three sampler VNA error model

Most compact VNA test set designs use three RF samplers. Two samplers connect to a backward wave coupler, one at each port, and the remaining typically connects to a power splitter placed just in front of the F/R switch. This third reference signal estimates the incident a_r at the stimulated port. Clearly, this setup inhibits the measurement of a_r at the unstimulated port and requires an error model which absorbs the load reflection Γ_b and Γ_a.

The used E-term error model, see fig. 2, consists of a disjunct forward and reverse six term error model. The signal flow diagram assumes a zero a_{r2} during forward mode. Conceptually, this chooses the port $r2$ reference impedance equal to the load impedance Z_b, and thus only a virtual b'_{r2} at Z_b is present. The transmission tracking E_{tf} absorbs the b_{r2}/b'_{r2} proportionality factor. Likewise, the load match E_{lf} is the error box b port 2 reflection with its port 1 terminated by Γ_b. The remaining terms, directivity E_{df}, reflection tracking E_{rf} and source match E_{sf}, are independent of source and load reflection. Analogous considerations are valid for the reverse measurement.

Correcting the measured ratios S_{F11}, S_{F21} and S_{R12}, S_{R22} must be done using the twelve E-term error model. These quantities differ from standard S-parameters since they are respectively for a Z_{r1}, Z_b and Z_a, Z_{r2} reference impedance system. The raw measurements are easily expressed in terms of the true S-parameters using the signal flow diagram. Inversion yields the wanted deembedding equations[8][1]. An alternative is to calculate the waves at the DUT for the forward and reverse measurement, and to solve (1). For the forward mode, the DUT waves follow from

$$\begin{bmatrix} a_1^F \\ b_1^F \end{bmatrix} = \frac{1}{E_{rf}} \begin{bmatrix} E_{rf} - E_{df}E_{rf} & E_{sf} \\ -E_{df} & 1 \end{bmatrix} \begin{bmatrix} a_{r1}^F \\ b_{r1}^F \end{bmatrix} \tag{6}$$

$$\begin{cases} b_2^F = b_{r2}^F/E_{tf} \\ a_2^F = E_{lf}b_2^F \end{cases} \tag{7}$$

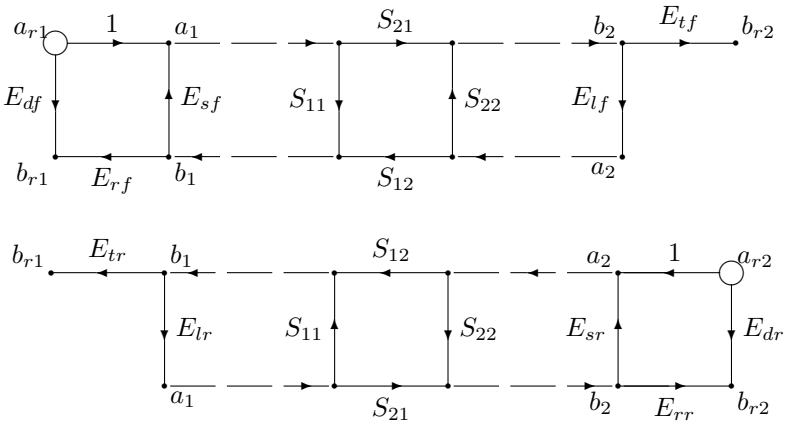

Figure 2: The 12 E-term error model consists of a disjunct forward, top, and reverse, bottom, error model. The two isolation terms E_{xf} and E_{xr} are not shown.

with the raw waves known up to a factor from

$$a_{r1}^F = 1 \qquad a_{r2}^F = 0 \tag{8}$$
$$b_{r1}^F = S_{F11} \qquad b_{r2}^F = S_{F21}\,. \tag{9}$$

Substituting f by r and exchanging the index 1 by 2 and 2 by 1 yields the equations for the reverse measurement.

Short-Open-Load-Thru is the only calibration method capable of determining the E-terms directly. The forward terms are calculated from forward stimulation only. First, three known reflection standards are measured at port 1. The three resulting equations allow for the calculation of E_{df}, E_{rf} and E_{sf}. Also, the isolation E_{xf} is typically associated with the leakage present when measuring the load standard. Then, a thru connection is measured. The corrected reflection, via (6), is E_{lf} and E_{tf} equals b_{r2}^F/a_1^F, as follows from (7) since $b_2^F = a_1^F$.

More advanced VNA test sets support error box based calibration like TLR and TMR/LRM. Most designs, e.g. the HP 8515a and 8517b, are four sampler three receiver hybrids. The test set consists of four samplers of which two connect to a backward wave coupler. The other two connect to a power splitter directly following the F/R switch so as to measure a_{r1} and a_{r2}. However, the VNA only detects three signals at a time, but the choice is independent of the stimulated port. Raw S-parameters are recovered in a two step process. First, two normal F/R measurements are done. Then, two additional F/R measurements are performed with the detectors respectively switched such that a_{r1}, a_{r2}, b_{r2} and a_{r2}, a_{r1}, b_{r1} are available. This yields the two load reflections $\Gamma_l = a_r/b_r$ at the unstimulated port. The switch term corrected raw S-parameters now follow from

$$S_r = \begin{bmatrix} S_{F11} & S_{R12} \\ S_{F21} & S_{R22} \end{bmatrix} \begin{bmatrix} 1 & S_{R12}\Gamma_a \\ S_{F21}\Gamma_b & 1 \end{bmatrix}^{-1} \tag{10}$$

using (2).

This slow twofold acquisition process is avoided by inclusion of the load reflections into the error box model. The resulting signal flow diagram, fig. 3, shows that Γ_b and Γ_a are defined relative to the reference impedance Z_{r2} and Z_{r1}. Thus, they only depend on the couplers, the F/R switch and the internal terminations, which are all highly stable. The effect of a source reflection is included in the measured a_r. As pointed out by[1], the internal port's load reflection may be ignored if the forward source and reverse load impedance is equal. Conceptually, the internal reference impedance is thus changed to this impedance, and its difference with Z_r is pushed into the port's error box.

The HP 8510c TLR calibration algorithm employs a variant of this approach. Each thru and line measurement is corrected for these switch terms via (10). The parameter "User3" is shown on the display during the additional nonstandard F/R measurements. Then, the seven parameter S-term error box model is calculated using the standard TLR algorithm. Finally, the backwards compatible twelve E-term model is calculated using the load reflections obtained from the thru measurement.

4 Calculating the switch terms

The E- and S-term signal flow diagrams, figures 2 and 3, are a mathematical representation of the same systematic error. Thus, the ten E-terms and the

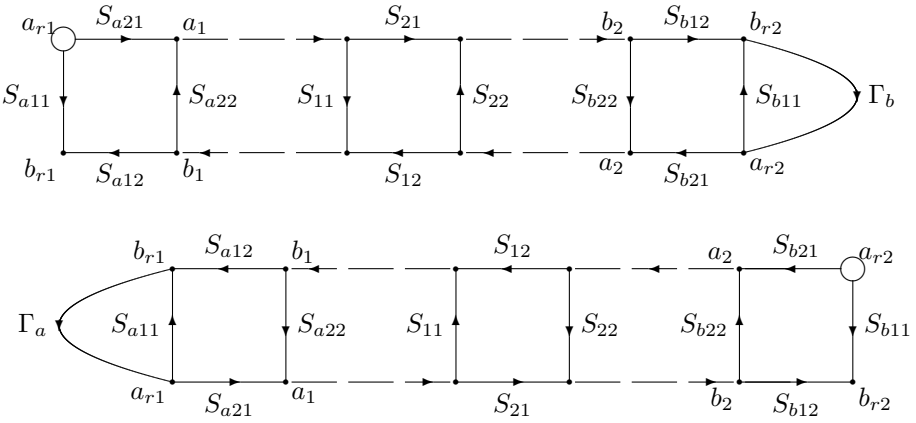

Figure 3: The signal flow diagram of the physical 8 S-term error box model for forward, top, and reverse, bottom, operation. The two switch terms Γ_b and Γ_a account for the load reflection of the unstimulated port.

seven parameters characterizing the S-term error box model, together with the two switch terms, comprise the same information.

A first relation follows from the requirement that the raw reflection calculated via both models must be equal when a zero transmission DUT is measured. From this condition, e.g. for the forward mode

$$S_{F11} = S_{r11} \Leftrightarrow \tag{11}$$

$$E_{df} + \frac{E_{rf}\Gamma_1}{1 - E_{sf}\Gamma_1} = S_{a11} + \frac{S_{a12}S_{a21}\Gamma_1}{1 - S_{a22}\Gamma_1} \tag{12}$$

with Γ_1 the true reflection at port 1, follows

$$E_{df} = S_{a11} \qquad E_{dr} = S_{b11} \tag{13}$$

$$E_{rf} = S_{a12}S_{a21} \qquad E_{rr} = S_{b12}S_{b21} \tag{14}$$

$$E_{sf} = S_{a22} \qquad E_{sr} = S_{b22}\,. \tag{15}$$

A second relation is obtained from the requirement that measuring a thru connection must yield the same S_{F11}, S_{F21} and S_{R12}, S_{R22} ratios. An elegant way of deriving the equations is by tracing the waves in the forward and reverse mode for both models. For the forward stimulation, this gives

$$\begin{bmatrix} a_1 \\ b_1 \end{bmatrix} = \overline{T}_f \begin{bmatrix} a_{r1} \\ b_{r1} \end{bmatrix} \tag{16}$$

$$\overline{T}_f = \frac{1}{E_{rf}} \begin{bmatrix} E_{rf} - E_{df}E_{rf} & E_{sf} \\ -E_{df} & 1 \end{bmatrix} \tag{17}$$

$$\frac{b_1}{a_1} = E_{lf} \tag{18}$$

$$\frac{b_{r2}}{a_1} = E_{tf} \tag{19}$$

for the E-term model, with $\overline{T}_f$ the right cascading wave matrix, and

$$\begin{bmatrix} a'_1 \\ b'_1 \end{bmatrix} = \overline{T}_a \begin{bmatrix} a_{r1} \\ b_{r1} \end{bmatrix} \tag{20}$$

$$\overline{T}_a = \frac{1}{S_{a12}} \begin{bmatrix} -\det(S_a) & S_{a22} \\ -S_{a11} & 1 \end{bmatrix} \tag{21}$$

$$\frac{b'_1}{a'_1} = S_{b22} + \frac{S_{b12}S_{b21}\Gamma_b}{1 - S_{b11}\Gamma_b} \tag{22}$$

$$\frac{b_{r2}}{a'_1} = \frac{S_{b12}}{1 - S_{b11}\Gamma_b} = \frac{b_{r2}}{S_{a21}a_1} \tag{23}$$

for the S-term model, with $\overline{T}_a = S_{a21}\overline{T}_f$. Repeating the above derivation for the reverse mode yields the conditions

$$E_{lf} = S_{b22} + \frac{S_{b12}S_{b21}\Gamma_b}{1 - S_{b11}\Gamma_b} = E_{sr} + \frac{E_{rr}\Gamma_b}{1 - E_{dr}\Gamma_b} \tag{24}$$

$$E_{tf} = \frac{S_{a21}S_{b12}}{1 - S_{b11}\Gamma_b} = \frac{S_{a21}}{S_{b21}} \cdot \frac{E_{rr}}{1 - E_{dr}\Gamma_b} \tag{25}$$

$$E_{lr} = S_{a22} + \frac{S_{a12}S_{a21}\Gamma_a}{1 - S_{a11}\Gamma_a} = E_{sf} + \frac{E_{rf}\Gamma_a}{1 - E_{df}\Gamma_a} \tag{26}$$

$$E_{tr} = \frac{S_{a12}S_{b21}}{1 - S_{a11}\Gamma_a} = \frac{S_{b21}}{S_{a21}} \cdot \frac{E_{rf}}{1 - E_{df}\Gamma_a} \tag{27}$$

when substituting (13–15). These equations are equivalent to [1, eqs. 36–39] but offer the computational advantage that they are equally valid for the special cases $\Gamma_b = 0$ and $\Gamma_a = 0$. Inversion gives

$$\Gamma_b = \frac{E_{lf} - E_{sr}}{E_{rr} + E_{dr}(E_{lf} - E_{sr})} \tag{28}$$

$$S_{a21}S_{b12} = E_{tf}(1 - E_{dr}\Gamma_b) \tag{29}$$

$$\Gamma_a = \frac{E_{lr} - E_{sf}}{E_{rf} + E_{df}(E_{lr} - E_{sf})} \tag{30}$$

$$S_{a12}S_{b21} = E_{tr}(1 - E_{df}\Gamma_a) \tag{31}$$

where the product of (29) and (31) is not guaranteed equal to $E_{rf}E_{rr}$ from (14). Consistency requires

$$E_{tf}E_{tr} = \frac{E_{rr}}{1-E_{dr}\Gamma_b}\cdot\frac{E_{rf}}{1-E_{df}\Gamma_a} \quad (32)$$

as follows from (25) and (27). A practical solution for an E- to S-term conversion algorithm is to choose a consistent estimate E_{tfe} and E_{fre} such that

$$e_{tfe} = \frac{E_{tfe}}{E_{tf}} \approx 1 \qquad e_{tre} = \frac{E_{tre}}{E_{tr}} \approx 1 \quad (33)$$

satisfying the constraint (32)

$$e_{tfe}e_{tre} = k = \frac{\frac{E_{rr}}{1-E_{dr}\Gamma_b}\cdot\frac{E_{rf}}{1-E_{df}\Gamma_a}}{E_{tf}E_{tr}}. \quad (34)$$

Solving (33–34) in least squares sense, by minimizing $\chi^2 = |e_{tfe}-1|^2 + |e_{tfr}-1|^2$, gives

$$e_{tfe} = e_{tre} = \sqrt{k}. \quad (35)$$

Defining a forward and reverse estimate of S_{a21}/S_{b21} via (25) and (27), and rewriting the ratio E_{tfe}/E_{tre} in terms of the consistent estimate S_{a21}/S_{b21} via the same equations, yields

$$\left(\frac{S_{a21}}{S_{b21}}\right)_e = \sqrt{\left(\frac{S_{a21}}{S_{b21}}\right)_f\left(\frac{S_{a21}}{S_{b21}}\right)_r}. \quad (36)$$

Thus, the proposed method averages using a geometric mean.

5 A nonzero length thru

SOLT calibration establishes the port 1 reference plane from three reflection standards measured during the forward stimulation. It further attributes the measured thru response to E_{lf} and E_{tf}. The same procedure during reverse mode sets the port 2 reference plane and yields E_{lr} and E_{tr}. Thus, if the port 1 and 2 reference planes do not coincide during the thru measurement, then anything in between them will be absorbed into the load and tracking terms. During forward mode, it is as if E_{lf} and E_{tf} are the result of a disturbance cascaded by S_b and terminated in Γ_b, from the reference plane "1" to "r2" in fig. 1. This effect may result from a different torque when joining both connectors, or from a thru measurement using a nonzero length standard.

Clearly, (13–21) are unchanged and the raw ratios S_{F11}, S_{F21} and S_{R12}, S_{R22} may still be calculated from the F/R E-term model, fig. 2, using a straight thru connection. However, these ratios must now be compared to the response of a S-term error box model with a nonideal thru present as DUT in fig. 3. Assuming a reflectionless thru characterized by a transmission $S_{t12} = S_{t21} = T = e^{-\gamma l}$ allows to map the ten E-terms to a seven parameter S-term model, two switch terms, and one offset error T. Reexamining (22–27) gives the same expressions, multiplied by a factor T^2 for E_l and T for E_t. Inversion yields

$$\Gamma_b = \frac{E_{lf}/T^2 - E_{sr}}{E_{rr} + E_{dr}(E_{lf}/T^2 - E_{sr})} \quad (37)$$

$$S_{a21}S_{b12} = E_{tf}/T\cdot(1-E_{dr}\Gamma_b) \quad (38)$$

$$\Gamma_a = \frac{E_{lr}/T^2 - E_{sf}}{E_{rf} + E_{df}(E_{lr}/T^2 - E_{sf})} \quad (39)$$

$$S_{a12}S_{b21} = E_{tr}/T\cdot(1-E_{df}\Gamma_a) \quad (40)$$

and the product of (38) and (40) becomes

$$E_{tf}E_{tr} = T^2\frac{E_{rr}}{1-E_{dr}\Gamma_b}\cdot\frac{E_{rf}}{1-E_{df}\Gamma_a}. \quad (41)$$

Substituting (37) and (39) into (41) yields a quadratic equation $aT^4 + bT^2 + c = 0$ with

$$a = \frac{(E_{rf}-E_{df}E_{sf})(E_{rr}-E_{dr}E_{sr})}{E_{tf}E_{tr}} \approx \frac{1}{T^2} \quad (42)$$

$$b = \frac{E_{dr}E_{lf}(E_{rf}-E_{df}E_{sf}) + E_{df}E_{lr}(E_{rr}-E_{dr}E_{sr})}{E_{tf}E_{tr}} - 1$$

$$\approx -1 \quad (43)$$

$$c = \frac{E_{dr}E_{lf}E_{df}E_{lr}}{E_{tf}E_{tr}} \approx 0 \quad (44)$$

where the approximations hold for low error box reflections, as is usually the case. Thus, the discriminant $b^2 - 4ac$ is close to unity, and the unphysical solution of T^2 is easily recognized as the one having the smallest magnitude. Also, the extracted load reflections will approximate (28) and (30). Furthermore, comparison of (34) with (41) shows that the quantities E_{tf}/T and E_{tr}/T approximate the optimal estimates presented in §4.

6 Including thru reflections

Most three detector systems employ a test set with a programmable attenuator inserted between the F/R with and each test port, see e.g. fig. 4. Thus, the switch terms will almost vanish if an attenuation of 20 dB or more is used. Assuming zero load reflections allows for the mapping of the ten E-terms into a seven parameter S-term model and a reciprocal nonideal thru characterized by three terms, S_{t11}, S_{t21} and S_{t22}.

Again, (13–21) are unchanged. Comparing the response of the straight thru connected F/R E-term

model and the S-term model with the nonideal thru present as DUT yields

$$E_{lf} = S_{t11} + \frac{E_{sr}S_{t21}^2}{1 - E_{sr}S_{t22}} \quad (45)$$

$$E_{tf} = \frac{S_{a21}}{S_{b21}} \cdot \frac{E_{rr}S_{t21}}{1 - E_{sr}S_{t22}} \quad (46)$$

$$E_{lr} = S_{t22} + \frac{E_{sf}S_{t21}^2}{1 - E_{sf}S_{t11}} \quad (47)$$

$$E_{tr} = \frac{S_{b21}}{S_{a21}} \cdot \frac{E_{rf}S_{t21}}{1 - E_{sf}S_{t11}} \quad (48)$$

which may be solved by first equating

$$E_{tf}E_{tr} = S_{t21}^2 \frac{E_{rr}}{1 - E_{sr}S_{t22}} \cdot \frac{E_{rf}}{1 - E_{sf}S_{t11}} . \quad (49)$$

Now, substituting S_{t21}^2 from (49) into (45) and (47) gives

$$S_{t11} = \frac{E_{lf}E_{rf}E_{rr} - E_{sr}E_{tf}E_{tr}}{E_{rf}E_{rr} - E_{sf}E_{sr}E_{tf}E_{tr}} \quad (50)$$

$$S_{t22} = \frac{E_{lr}E_{rf}E_{rr} - E_{sf}E_{tf}E_{tr}}{E_{rf}E_{rr} - E_{sf}E_{sr}E_{tf}E_{tr}} \quad (51)$$

from which S_{t21}^2 follows. The S-term error box model can now be completed via the ratio S_{a21}/S_{b21}. Also, recalculating the load and tracking terms for an ideal thru yields the SOLR E-terms if a SOLT calibration was performed.

7 Practical test set behaviour

The suitability of the presented methods is verified by inspection of the E-terms after LRM and SOLT calibration. Especially the effect of different attenuator settings on the extracted load reflections provides some insights.

Figure 4 shows the block diagram of the used test set. Each output of the F/R switch is followed by a built-in power splitter. One output connects to an attenuator, a backward wave coupler, and finally the VNA test port. The other output provides a reference signal via a taper. All peripheral components are assumed ideal reciprocal reflectionless in a constant system reference impedance Z_r.

A three by three S-parameter matrix, see fig. 4 for the port numbering, describes the power splitter. Expressing $V_3^-(V_2^+, V_2^-, V_3^+)$ and substituting

$$V_2^+ = Ab_t \quad V_2^- = \frac{a_t}{A} \quad V_3^+ = 0 \quad a_r = TV_3^- \quad (52)$$

into this linear relation yields the first identity

$$\delta_s = S_{32} - \frac{S_{22}S_{31}}{S_{21}} \quad (53)$$

$$a_r = \frac{S_{31}}{S_{21}} \cdot \frac{Ta_t}{A} + \delta_s TAb_t \quad (54)$$

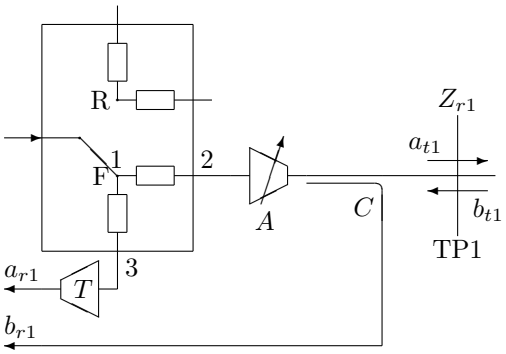

Figure 4: The simplified HP 8515a block diagram. The harmonic RF/IF mixers, also called Grove samplers, the DC bias tees and the port 2 circuits are not shown.

with the leakage δ_s zero for an ideal splitter, since it is then reciprocal and characterized by

$$S_{11} = 0 \qquad S_{21} = S_{31} = 0.5 \quad (55)$$

$$S_{32} = 0.25 \qquad S_{22} = S_{33} = 0.25 . \quad (56)$$

The second identity, assuming an ideal coupler, is

$$b_r = Cb_t \quad (57)$$

which completes the test set model. In forward mode, the measured raw port 1 reflection now becomes

$$\Gamma_r = \frac{b_r^F}{a_r^F} = \frac{AC}{T\left(\frac{S_{31}}{S_{21}\Gamma_t} + \delta_s A^2\right)} \quad (58)$$

with Γ_t the DUT reflection at the test port. In reverse mode, the measured load reflection is

$$\delta_l = S_{22} + \frac{S_{12}S_{21}\Gamma_L}{1 - S_{11}\Gamma_L} \quad (59)$$

$$\Gamma_l = \frac{a_r^R}{b_r^R} = \frac{AT}{C}\left(\delta_l \frac{S_{31}}{S_{21}} + \delta_s\right) \quad (60)$$

where $\Gamma_L \approx -1$ is the reflection presented at the splitter port 1 by the switch.

For an ideal system, lowering the transmission A scales E_r and Γ_l proportionally, as follows from (58) and (60), and reduces the reflection at the test port to $A^2\delta_l$. Thus, choosing high attenuation removes the switch terms. It will, however, not necessarily improve final accuracy due to the detector's limited dynamic range.

This idealized model allows to relate the unphysical raw waves and physical waves at the test port reference plane. The virtual two-port obeys

$$\begin{bmatrix} b_r \\ a_r \end{bmatrix} = \begin{bmatrix} C & 0 \\ \delta_s TA & \frac{S_{31}T}{S_{21}A} \end{bmatrix} \begin{bmatrix} b_t \\ a_t \end{bmatrix} \quad (61)$$

which is a left cascading wave matrix equation of an error box. The equivalent S-parameters are

$$S_x = \begin{bmatrix} 0 & C \\ \frac{S_{21}}{S_{31}}\frac{A}{T} & -\frac{S_{21}}{S_{31}}\delta_s A^2 \end{bmatrix}, \quad (62)$$

which reveals their dependence on the test set properties.

8 Experiment

The HP 8510c VNA was set up with an HP 8515a 26.5 GHz test set. A step mode frequency sweep was performed with an IF averaging of 64. All test interfaces are 3.5 mm coaxial, with test port 1 male and port 2 female. After calibration, the VNA internal E-terms were stored on disk for further processing.

The system was LRM calibrated using a HP 85052c high precision mechanical calibration kit. The extracted values obtained from the method in §5 show the expected behaviour, see fig. 5. A proportional decrease of the reflection tracking E_{rf} and error box load reflection Γ_b is observed when increasing the attenuation from 0 to 10 dB. For the 0 dB case, the thru transmission S_{t21} is not exactly unity as would be expected. Its root-mean-square difference from unity is $3 \cdot 10^{-4}$. Clearly, the VNA's internal S- to E-term conversion algorithm employs extra correction terms which are not present in the error box model of fig. 3, or measures some terms used in the expressions (24–27) directly, instead of calculating them from the load reflections. Almost equal results were obtained from the standard method in §4. The absolute and relative rms difference on the recovered load reflections were $3 \cdot 10^{-5}$ and 0.01 dB, respectively. The two estimates $S_{a21}S_{b12}$, from (29) and (38), differed by $4 \cdot 10^{-4}$ or 0.003 dB.

A SOLT calibration was performed using a standard HP 85052d economy calibration kit. The extracted load reflection, see fig. 5, unphysically increases with the port's attenuator setting. Clearly, the error box model with a reflectionless thru is not valid. The noisy reflection data for the 0 dB case, as if it is a vectorial sum of two spatially separated reflections, and its increase with attenuation indicates that the thru own reflection may not be neglected.

The method presented in §6 assumes zero switch terms and extracts the thru transmission and reflections. The extracted data for the 0 dB case, see fig. 6, is noisy and may result from the superposition of thru and load reflections. Increasing attenuation to 10 dB removes most noise. Moreover, the now recovered thru reflection is almost unchanged. This independence supports the assumption that the thru is causing most E- to S-term model inconsistency. Note that the thru reflection also consists of differences between the female and male SOL standards. The transmission phase reveals a coaxial reference plane error of about 30 μm.

9 Conclusion

Most commercial two port VNAs allow for the measurement of only three waves at a time. Thus, the unstimulated port termination is unknown and must be included in the error model. The used twelve E-term model can be converted into a physical S-term model and switch terms modelling this effect. Three methods based on different assumptions are presented. Experimental data agrees with the physical test set construction.

Acknowledgment

This work was supported by the Institute for the Promotion of Innovation by Science and Technology in Flanders (IWT) and the Interuniversity Micro-Electronics Center (IMEC). D. Schreurs is supported by the Fund for Scientific Research (FWO).

References

[1] R.B. Marks, "Formulations of the Basic Vector Network Analyzer Error Model Including Switch Terms," *50th ARFTG Conference Digest,* December 1997, pp. 115–126.

[2] G. Engen, C. Hoer, "Thru-Reflect-line: An Improved Technique for Calibrating the Dual Six-Port Automatic Network Analyzer," *IEEE Transactions on Microwave Theory and Techniques,* Vol. 27, No. 12, December 1979, pp. 987–998.

[3] R. Pantoja, M. Howes, J. Richardson, R. Pollard, "Improved Calibration and Measurement of the Scattering Parameters of Microwave Integrated Circuits," *IEEE Transactions on Microwave Theory and Techniques,* Vol. 37, No. 11, November 1989, pp. 1675–1680.

[4] R.B. Marks, "A Multiline Method of Network Analyzer Calibration," *IEEE Transactions on Microwave Theory and Techniques,* Vol. 39, No. 7, July 1991, pp. 1205–1215.

[5] H.J. Eul, B. Schiek, "Thru-Match-Reflect: one result of a rigorous theory for de-embedding and network analyzer calibration technique," *Proc. of the 18th European Microwave Conference,* Stockholm, Sweden, September 1988, pp. 909-914.

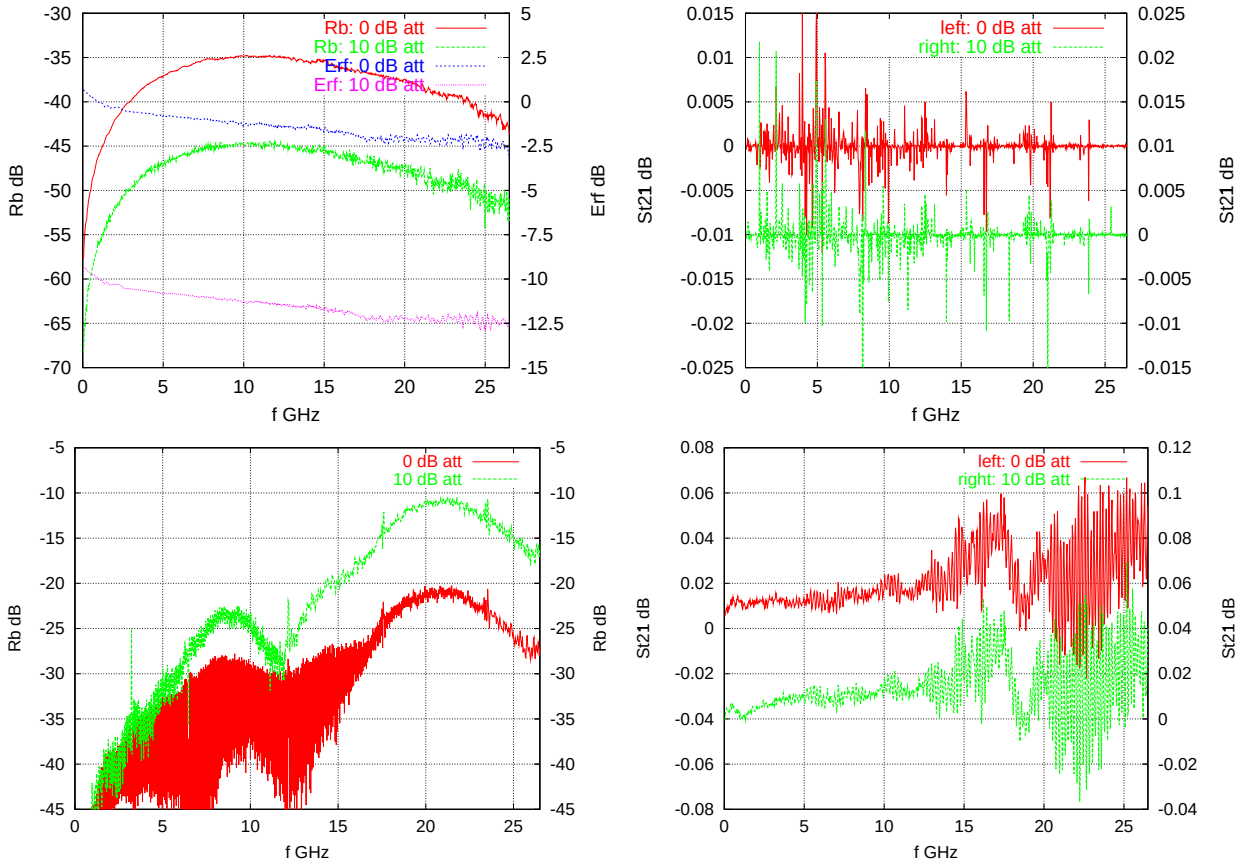

Figure 5: Top: the error box load reflection Γ_b and reflection tracking E_{rf}, left, and the thru transmission, right, extracted from the VNA E-terms. Two LRM calibrations with an attenuator setting of 0 and 10 dB were used. Bottom: the error box load reflection Γ_b, left, and the thru transmission, right, extracted from two SOLT calibrations with an attenuator setting of 0 and 10 dB. The load reflection unphysically increases with attenuation.

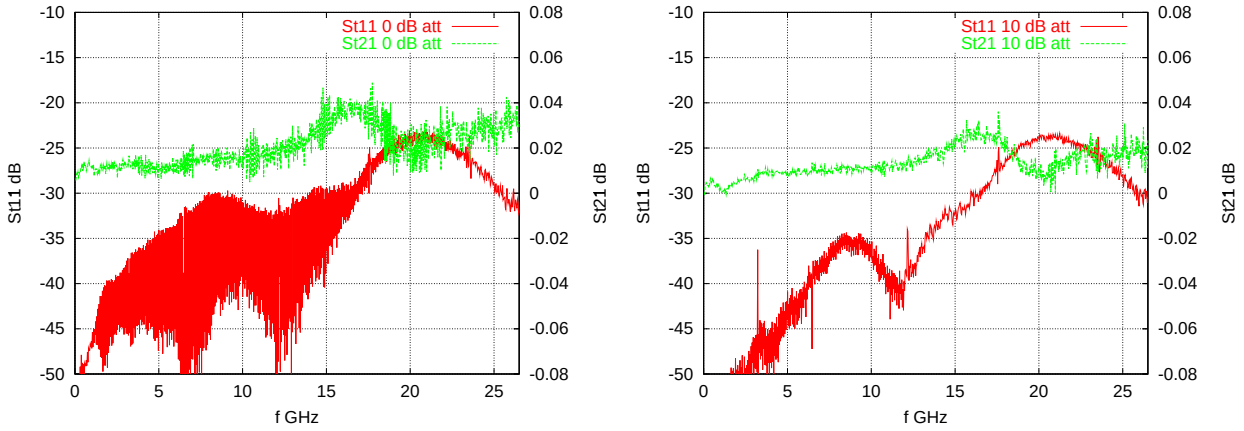

Figure 6: The thru reflection and transmission extracted from an E-term error model obtained after SOLT calibration. The noisy data for the 0 dB attenuator setting, left, may result from a superposition of thru and switch term reflections. The 10 dB attenuation result, right, approximates the 0 dB data except for the noise.

[6] A.F. Ferrero, "Two-port network analyzer calibration using an unknown thru," *IEEE Microwave and Guided Wave Letters,* Vol. 2, No. 12, December 1992, pp. 505–507.

[7] S. Vandenberghe, D. Schreurs, G. Carchon, B. Nauwelaers, W. De Raedt, "S-parameter Reciprocity Relations, Normalization, and TLR Error Box Completion," *Int J RF and mm-wave CAE,* John Wiley & Sons, Inc., vol. 12, no. 5, 2002, pp. 418–427.

[8] D. Rytting, "An Analysis of Vector Measurement Accuracy Enhancement Techniques," *RF & Microwave Symposium and Exhibition,* 1980.